Drilling of micron-scale high aspect ratio holes with ultra-short pulsed lasers:

Nasrollahi, Vahid; Penchev, Pavel; Jwad, Tahseen; Dimov, Stefan; Kim, Kyunghan; Im, Changmin

DOI:
10.1016/j.optlaseng.2018.04.024

Drilling of micron-scale high aspect ratio holes with ultra-short pulsed lasers: critical effects of focusing lenses and fluence on the resulting holes' morphology

Vahid Nasrollahi[a]*, Pavel Penchev[a], Tahseen Jwad[a], Stefan Dimov[a], Kyunghan Kim[b], Changmin Im[c]

[a] Department of Mechanical Engineering, University of Birmingham, Edgbaston, Birmingham B15 2TT, UK

[b] Korea Institute of Machinery & Materials, Daejeon 34103, South Korea

[c] SDA Company Ltd, 38-16, Ojeon-dong, Uiwang-City, Kyunggi-Do, South Korea

* Corresponding author, Email: vxn342@bham.ac.uk

Abstract

Micro drilling employing ultra-short pulsed lasers is a promising manufacturing technology for producing high aspect ratio holes, particularly on ceramic substrates due to the growing range of application in electronic industry. Controlling the morphology and quality of the holes is an important factor in fulfilling the requirements of such applications. In this research, the effects of a wide fluence spectrum associated with the use of femto-second lasers on achievable aspect ratios were investigated by employing lenses with different focal distances. The holes' morphology and quality were analysed utilising a high resolution X-ray tomography (XCT). It was demonstrated that the achievable aspect ratio can be increased from 3 to 25 just by varying the lenses focal distances. In addition, the quality of produced holes in terms of taper angle and cylindricity was investigated and the results showed that the quality would be improved by increasing the fluence and/or decreasing the focal distance. At the same time, the limitations of drilling holes with low focal distance lenses were discussed, i.e. sensitivity to defocusing and increased risks of recast formations inside the holes and bending effects, that should be considered in designing processes for high aspect ratio percussion drilling.

Keywords: Laser microdrilling; hole morphology; high aspect ratio holes; focusing lenses.

1. Introduction

The trend toward product miniaturisation and thus for manufacturing micro scale functional features and components demand new tools, methods and also a better understanding of materials' behaviour at such scales [1]. High aspect ratio (depth to diameter ratio) micro holes are common features in products, e.g. the channels for delivering media in micro-electromechanical systems (MEMS), nozzles for diesel fuel injection, cooling channels for turbine blades, drug delivery orifices, etc. [2-4]. Different methods have been used for producing such holes, in particular photo-etching, electro-chemical machining, electro-discharge machining and laser drilling, and their capabilities and limitations have been investigated by researchers [3, 5]. One of these technologies, particularly ultra-short pulsed laser drilling, has attracted a significant interest due to its non-contact nature and efficiency in producing micro-scale holes in almost any material [1]. Another advantage of this method is the possibility to control inner surface topology and thus to tune its properties by generating laser induced periodic surfaces structures (LIPSS). In particular, it is possible to control hydrophobicity of the holes that can be of interest to automotive industry, e.g. to decrease the risk of coking deposition and nozzle clogging [6, 7].

Another important and growing application area for high aspect ratio micro holes is in electronic industry, i.e. interconnecting vias of printed circuit boards and guide blocks of interface probe cards for testing 3D integrated circuits and electronic devices [8-11]. In particular, it is necessary in such applications to produce arrays of holes usually in ceramic substrates with aspect ratios more than 5 while their diameters and pitches are less than 60μm and taper angle does not exceed 10°. Also, such arrays of holes should fulfil stringent requirements in regards to their accuracy, repeatability and processing speed that introduce further constraints and thus limit the available options for their cost effective manufacture.

Moreover, considering the growing demand for drilling micro holes with diameters down to 10µm, laser micro drilling is becoming even a more attractive option that potentially can fulfil these requirements.

At the same time, the laser micro drilling process has some limitations, i.e. the achievable aspect ratios, holes tapering, circularity deviations, a heat affected zone (HAZ), spatters, recast formations and micro cracks. They are more pronounced in stationary beam drilling methods such as percussion drilling, compared with lower throughput, moving beam methods like trepanning and helical drilling [12]. To address these issues, for both drilling categories, new methods and tools have been developed, in particular changing the focusing position [8, 13], the use of assisted gases [14-17], beam rotation [18, 19], drilling under water [20], two-side drilling [21, 22], new drilling cycles [12] and also different modelling and optimizing approaches to identify the optimum processing window [23-27]. Furthermore, the effects of process settings were investigated, too, especially peak power and pulse width effects on holes' repeatability in regards to the entry diameters [28] the evolution of shallow craters' diameter and depth in regards to number of pulses (NoP) and fluence [29] and the effect of different laser parameters such as average power on circularity, HAZ and taper angle [30]

Other parameters that affect the laser drilling process, especially pulse energy, fluence and intensity, have been investigated, too. For instance, how the laser intensity at three different wavelength affects the drilling rate [31]. Also, pulse duration effects in the nano-second range and laser intensity on drilling speed was investigated and a conclusion was made that the melt expulsion was the most efficient material removal mechanism in this regime [32]. These three process parameters have an impact on holes' quality, too, especially on their circularity, edge definition and taper angles [33, 34]. However, it should be noted that these conclusions are predominantly based on analysis of thin plates' surfaces after the drilling operations or just on morphology of shallow dimples. In addition, it should be noted that the maximum achievable

depth, holes' aspect ratio and the ways to increase it in ultra-short pulsed drilling have not been studied and this applies to all materials including ceramics.

This research, by employing lenses with different focal distance, reports an investigation into the effects of a wide fluence spectrum in ultra-short percussion drilling on achievable holes' aspect ratio and quality. The morphology of the holes in terms of cylindricity and taper angle was investigated in details by employing a high resolution XCT system. The limitations of using lower focal distance lenses were also analysed, especially their depth of focus, recast formations inside the holes and bending effects that should be considered in designing percussion drilling processes for such lenses.

2. Materials and Methods

2.1. Experimental and measurement setups

Silicon nitride (Si_3N_4) wafers with a material specification to meet the requirements of a wide range of application in microelectronic and microelectromechanical systems, i.e. resistance in high-energy manufacturing processes and insulation capabilities, were used in the research [35]. The thickness of the substrates was 250µm and their surface roughness (Sa) was 220nm, measured with a focus variation microscope (Alicona G5).

A 5 W Yb-doped sub-pico laser source with pulse duration of 310fs, beam quality factor (M2) better than 1.3, 1030nm wavelength and pulse frequencies up to 500kHz from Amplitude Systems was used in this research. The beam delivery system includes a quarter-wave plate to obtain a circular polarisation and exchangeable focusing lenses, in particular to use 100, 50 and 20 mm focal distance lenses. To maintain the focal distance with high accuracy and repeatability, the lens was mounted on a mechanical Z stage with positional resolution of

500nm while the workpiece was mounted on a stack of high precision X and Y mechanical stages with resolution of 250 nm.

A percussion drilling strategy was employed in this research and the focal position was maintained the same during the processing. The pulse frequency used in the experiments was 100kHz. It should be noted that this pulse frequency was selected by conducting some initial trials while the maximum achievable pulse energy with the used laser source was utilised. In particular, through these trials the trade-offs between holes' quality, i.e. the recast formation, and processing speed that affect directly the achievable penetration depth were considered and thus to identify the optimum pulse frequency for the used laser source and substrate material.

A range of inspection methods to characterise laser drilled high aspect ratio holes, i.e. optical instruments and producing replicas of the holes by infiltrating liquid PMMA into the holes under vacuum conditions, were considered but was concluded that they did not provide sufficient insight into the process and therefore were not used in this research. Also, destructive methods as cutting and then grinding the cross sections of the samples were examined, too. It was judged that they would introduce uncertainty in the inspection process that would be in order of difference of compared measurands and therefore would not meet the requirements of this experimental study. Taking into account the limitations of these non-destructive and destructive inspection methods, high resolution X-ray tomography was selected to assess the depth and morphology of the laser drilled micro-holes. In particular, a Zeiss XRADIA Versa XRM-500 system was employed in this research. The measurements settings selected to minimise the measurement uncertainly, especially the acceleration voltage, current and exposure time for each projection were set to 50 kV, 79 μA and 7 s, respectively. In this way projection images of 1013 by 1013 pixels were used to reconstruct the volumes of the drilled substrates over a grid of 1 μm cubic voxels. Then, this data set was analysed employing VG

studio 3.0 from Volume Graphics and the surface model was defined by applying the VG's advanced surface determination, starting with the ISO 50 surface determination.

2.2. Design of experiments

To compare the laser drilling results obtained with three different lenses in terms of drilling rate and optimum NoP after which the penetration rate decreases substantially (referred to as a saturation point), arrays of blind holes with varying NoP were produced with three lens. The NoP range was selected to cover the early stages of the hole formation before the saturation point is reached and also beyond. i.e. 100, 500, 1000, 1600, 2000, 2500, 5000, 10000 and 15000. The maximum pulse energy achievable with the used laser source i.e. 9 µJ was used in this experiment and each combination of drilling settings was repeated 7 times to assess repeatability and reliability of the results obtained in this research.

Next, the effects of a wide fluence spectrum were assessed by employing three different lenses with focal distances of 100, 50 and 20 mm and beam diameters of 45, 23 and 9µm (measured using a beam profile analyser of Dataray Beam R2), respectively. The fluence ranges achieved for each lens by utilising the full range of pulse energies available with the used laser source are shown in Table 1. The highest fluence levels for the three lenses were different as a result of their different beam spot diameters while utilising the maximum deliverable pulse energy for the used laser source, i.e. 9µJ. Hence, the same fluence for the three lenses can be obtained by decreasing the pulse energy and thus to investigate a wider spectrum of fluence effects on the percussion drilling process. The lowest level of fluence for each lens was selected taking into account the silicon nitride ablation threshold, 0.24 J/cm^2, calculated experimentally using Liu's method [36]. Thus, employing the three lenses all the experiments were carried out with 1,000 and 10,000 pulses to examine the fluence effects, both

before and after the saturation point. Again, the experiments for each set of parameters were repeated 7 times.

2.3. Depth of focus analysis

The issues associated with off-focus processing are common in laser machining but they could be ignored if their effects are negligible. However, lenses with small focal distances are sensitive to defocusing and consequently require fine adjustment in Z direction [37]. Therefore, higher resolution stages and sensors for setting up the focal plane are necessary for such lenses and this can have an impact on process flexibility and also increases the setup cost. The term, depth of focus (DOF), can be used to assess the sensitivity of a given laser machining setup to off-focus processing. As a laser beam with a Gaussian energy profile is employed in this research, the theoretical DOF can be calculated using Eq (1).

$$DOF = \frac{8\lambda}{\pi}\left(\frac{f}{D}\right)^2 \cdot M^2 \quad (1)$$

where: λ is the wavelength of the laser beam, f - the lens focal distance and D is the input beam diameter at the lens.

Thus, the theoretical DOF of the 100, 50 and 20 mm lenses calculated using Eq (1) are 2375µm, 621µm and 95µm, respectively. There is a substantial DOF reduction when lenses with small focal distances are used and therefore their sensitivity to off-focus processing was analysed in this research. Therefore, additional experiments were carried out with a defocused beam, especially ±50µm, ±100µm and ±200µm, for all three lenses. The pulse energy in these experiments was fixed at 9µJ while NoP were kept at 500 and 5,000 to examine the effects both, before and after the saturation point. Again, as in all experiments in this research each process setting was repeated 7 times to assess the reliability of the obtained results.

3. Results and Discussion

3.1. Saturation point

The capabilities of the three lenses in regards to achievable aspect ratios in percussion laser drilling of micro holes were examined in these first series of experiments. The arrays of blind holes produced with each lens by varying NoP were analysed by extracting the cross sectional views from the XCT results as depicted partly in Figure 1 for the holes drilled using 500, 1000, 5000 and 10000 pulses with 3 repetitions in each case. It can be clearly seen that the penetration stops at the early stages when the 100 mm lens was employed. The functional dependence between NoP and achievable penetration depth for the three lenses is given in Figure 2. It highlights clearly the benefits of employing lenses with smaller focal distances and thus to achieve higher fluence. The saturation point for the 100mm lens was below the 110 μm mark while it was increased to 152 and 200 μm for 50 and 20 mm lenses, respectively. In all cases, any further increases of NoP after the saturation point did lead only to small improvements in regards to the achieved penetration depth.

The decrease of the drilling rates have been attributed to different factors such as plasma shielding and the angular dependence of laser absorption. In this research, the increase of the holes' surface area during the drilling process that led to a decrease of the effective fluence were considered a dominant factor in limiting the penetration depth [38]. This phenomenon is consistent across all three lenses, however since the fluence was much closer to the ablation threshold when the 100mm lens was employed the saturation occurred in early stages of the drilling process.

3.2. Fluence effects

The effects of fluence on achievable depth when employing the three different lenses was investigated by completing the experiments described in Table 1. The results obtained for the two different NoP used in the experiments are provided in Figure 3. It shows clearly how the increase of fluence affects the achievable penetration depth for each lens. This trend is more pronounced for the lenses with a bigger focal distance. At the same time, the lenses with a smaller focal distance can cover wider fluence ranges and thus to maintain the effective fluence at higher levels for longer that translates in a higher penetration depth. This is very well pronounced when 10,000 pulses were used, especially the penetration depth increases from 134 μm for the 100mm lens to 183 μm and 245 μm for the 50 and 20 mm lenses, respectively.

If the achievable penetration depth with the same fluence levels of 1.4J/cm^2 with 10,000 pulses are compared for 20 and 50 mm lenses, i.e. 25 and 120 μm, respectively, there is a sharp increase. The same was observed when the depths achieved with 0.55J/cm^2 employing the 50 and 100 mm lenses were compared, especially an increase from 29 to 134 μm, respectively. This should be attributed to the high pulse energies used to achieve the same fluence levels as shown in Table 1 and this is in line with the results reported by Doring et.al. [39]. Another factor that contributes to the increase of the penetration depth is the bigger entry diameter of the holes drilled by the lenses with bigger focal distances (see Figure 1) as this facilitates the evacuation of the ablated material. Therefore, if these results are used to analyse the functional dependence between the fluence and achievable aspect ratios, as shown Figure 4, the same increasing trend can be observed. In particular, the increase of achievable aspect ratios was from 3 for the 100mm lens to 8 and 25 for the 50 and 20 mm lenses, respectively, when 10,000 pulses were deployed.

3.3. Depth of focus analysis

The use of lenses with smaller focal distances is an attractive option for drilling higher aspect ratio micro holes but requires a careful analysis of their sensitivity to potential off-focus processing. The results obtained for the conduced DOF analysis with 500 and 5,000 pulses described in Section 2.3 are provided in Figure 5 and depicts the same trend before and after the saturation point. While only negligible differences between the penetration depths were observed with the 100mm lens when the beam was defocused up to ±200µm the differences are much more pronounced for the 50mm lens, especially the penetration depth achieved with 5,000 pulses dropped approximately 24% (from 180 to 136 µm). The results obtained with the 20 mm lens are distinctly different and show a higher sensitivity to off-focus drilling. In particular, the penetration depth achieved with 5,000 pulses after only a small defocusing of +50 µm dropped from 232 to 149 µm, approximately 36%, that was less than the depth achieved with the 50mm lens. A further defocusing of +100µm and +200µm resulted in a drop of the hole depth to 80 µm (65% drop) and 34 µm (85% drop), respectively, that was less than the achieved depth with the 100mm lens. The main reason for this sharp drop is the large divergence angle of the beam that leads to a significant fluence drop. In particular, the beam radius in focus (ω_0) can be calculated as follows:

$$\omega_0 = \frac{2\lambda \cdot f \cdot M^2}{\pi \cdot D} \tag{2}$$

By applying some defocusing of z, beam radius would change to:

$$\omega(z) = \omega_0 \sqrt{1 + \left(\frac{M^2 \cdot \lambda \cdot z}{\pi \cdot \omega_0^2}\right)^2} \tag{3}$$

And, also the fluence due this z defocusing changes as follows:

$$F(z) = \frac{E}{\pi \omega(z)^2} = \frac{4\pi \cdot E \cdot f^2 \cdot D^2}{16\lambda^2 \cdot f^4 \cdot (M^2)^2 + \pi^2 \cdot D^4 \cdot z^2} \tag{4}$$

where: E is the pulse energy.

Substituting Eqs (2) and (3) in Eq (4), the first derivative of F(z) is:

$$\frac{dF(z)}{dz} = \frac{-8\pi^3 \cdot E \cdot D^6 \cdot z \cdot f^2}{(16\lambda^2 \cdot f^4 \cdot (M^2)^2 + \pi^2 \cdot D^4 \cdot z^2)^2} \quad (5)$$

Eq (5) shows how the rate of the fluence changes as a result of the beam defocusing dependence on the lenses' focal distance. Thus, the rate of fluence drop ($\frac{dF}{dz}$) in this study with a defocusing of 10 µm would be -115, -0.511 and -0.008 J/cm^2 per mm for the 20, 50 and 100 mm lenses, respectively, that explains the substantial effect of defocusing when lenses with smaller focal distances are used.

The beam divergence and spatial beam profiles of all three lenses calculated using Eq (3) that result from four different defocusing values are provided in Figure 6. The Gaussian beam spatial profile of the 20 mm lens for z = 0 has a sharp peak that is much higher than those of other two lenses and also the ablation threshold of silicon nitride, i.e. 0.24 J/cm^2. By applying 200 µm defocussing, the maximum fluence is for the 50 mm lens. Further increase of defocusing to 1,000 µm results in a complete reverse fluence order, especially the 100mm lens taking the top spot. However, it should be noted that in such high off-focus processing most of the beam spatial profiles of the 50 and 100 mm lenses are less than the silicon nitride ablation threshold while for the 20mm lens it is completely under the threshold line.

The other phenomenon regarding the 20 mm lens that is clearly pronounced in Figure 5 is the big discrepancy between the achieved penetration depths when positive and negative defocusing is applied, i.e. 222 µm compared with 149 µm when -50 µm and +50 µm defocusing was used in case of 5,000 pulses. The difference is maintained for -100 and +100 µm off-focus drilling, too, i.e. 142 and 80 µm, respectively. This could be explained with the effects of the increasing distance between the focus and the holes' bottom, when a positive defocusing was applied. Thus, it could be expected that a negative defocusing could lead to better results than laser drilling in focus; however, for percussion drilling with the 20 mm lens this was not the case as shown in Figure 5. The reason for this is that the beam defocusing leads to a substantial

fluence reduction accompanied with a significant change of the beam spatial profile that increases substantially the “filtered out” pulse energy in the drilling process as depicted in Figure 7. Thus, the use of negative defocusing is not effective in percussion laser drilling with small focal distance lenses.

3.4. Hole morphology

So far the focus was on the achievable penetration depth but the effects on holes’ morphologies (see Figure 1) should be discussed, too. It is clear that the NoP increase does not affect holes’ entry diameters. Also, it is apparent that lenses with a higher focal distance produce holes with bigger openings due to their bigger focal spot diameter. The other option available to drill holes with bigger diameters is the use of trepanning or helical drilling but this would have a high impact on achievable processing speed compared to percussion drilling. In addition, it should be noted that the implementation of helical drilling employing scan heads requires the use of telecentric lenses to keep the beam normal to the substrate surface and also to prevent any defocusing when moving the beam. However, telecentric lenses are available only with relatively bigger focal distances, e.g. 70 or 100 mm, due manufacturing constrains [40]. Also, it is possible to produce holes with bigger diameters by defocusing, however as it is shown in Section 3.3 it is not easy to set up the drilling process due to high sensitivity to off-focus processing. So, there is less flexibility in regards to the resulting holes’ diameters when percussion drilling strategies are used and therefore the focusing lens should be selected very carefully taking into account the targeted hole diameter, aspect ratio, and processing speed.

The other common morphological issue is the cone shape entry with a necking that leads to deep narrow holes as shown in Figure 1, especially 42 and 28 μm for the holes

produced with the100 and 50mm lenses using 5,000 pulses, respectively. At the same time, high aspect ratio uniform cylindrical holes were produced with the 20 mm lens. The average taper angles of the holes after 10,000 pulses were 9°, 4° and 1° for the 100, 50 and 20 mm lenses, respectively.

It should be stressed that recasts inside high aspect ratio hole are more likely to occur when lenses with a small focal distance are used because of the poor evacuation of the ablated material, in particular approximately 5% of the holes produced with the 20mm lens had such issues as shown in Figure 8a. The other problem of high aspect ratio holes is the bending effect, however only 3% of the holes produced with the 20mm lens exhibited such an effect as depicted in Figure 8b. One of the reasons for this phenomenon is the beam deflection by the ablated materials or the formed vapour cloud [41] that are more likely to occur in high aspect ratio holes.

4. Conclusions

The effects of a wide fluence spectrum in ultra-short percussion drilling with different focal distance lenses are reported in this research. Especially, the effects on achievable aspect ratios and morphologies of the micro holes produced in Silicon nitride substrates were investigated. Based on the obtained results the following conclusions were made:

- Generally, the achievable holes' aspect ratio can be increased by employing lower focal distance lenses. In particular, aspect ratios up to 25 was achieved with the maximum pulse energy available, 9µj, by using the 20 mm lens compared with only 8 and 3 for 50 and 100 mm lenses, respectively.
- Holes with much better cylindricity and lower taper angle can be percussion drilled with smaller focal distance lenses. In particular, the taper angle decreased from almost 9° to

less than 1° when the lens focal distance was reduced from 100 to 20 mm. In addition, lenses with smaller focal distance led to a substantial reduction of the resulting cone shape entries with necking.

- Both, the use of high fluence and high pulse energy lead to a high penetration depth.
- There are some limitations associated with the use of smaller focal distance lenses, i.e. smaller beam focal spot diameters and a higher sensitivity to defocusing. In addition, when such lenses are used to produce high aspect ratio holes the risks for recast formations inside the holes and the bending effects increase.

Acknowledgment

The research reported in this paper was supported by Korea Institute for Advancement of Technology (KIAT), i.e. the project on "Laser Machining of Ceramic Interface Cards for 3D wafer bumps", and two H2020 Factory of the Future projects, "Modular laser based additive manufacturing platform for large scale industrial applications" (MAESTRO) and "High-Impact Injection Moulding Platform for mass-production of 3D and/or large micro-structured surfaces with Antimicrobial, Self-cleaning, Anti-scratch, Anti-squeak and Aesthetic functionalities" (HIMALAIA). The authors would like to acknowledge the contribution of Martin Corfield and Lars Korner from the University of Nottingham in carrying out the XCT measurements.

References

[1] Y. Qin, A. Brockett, Y. Ma, A. Razali, J. Zhao, C. Harrison, W. Pan, X. Dai, D. Loziak, Micro-manufacturing: research, technology outcomes and development issues, The International Journal of Advanced Manufacturing Technology, 47 (2010) 821-837.

[2] E. Ferraris, V. Castiglioni, F. Ceyssens, M. Annoni, B. Lauwers, D. Reynaerts, EDM drilling of ultra-high aspect ratio micro holes with insulated tools, CIRP Annals - Manufacturing Technology, 62 (2013) 191-194.
[3] Z.Y. Yu, Y. Zhang, J. Li, J. Luan, F. Zhao, D. Guo, High aspect ratio micro-hole drilling aided with ultrasonic vibration and planetary movement of electrode by micro-EDM, CIRP Annals - Manufacturing Technology, 58 (2009) 213-216.
[4] C. Diver, J. Atkinson, H.J. Helml, L. Li, Micro-EDM drilling of tapered holes for industrial applications, Journal of Materials Processing Technology, 149 (2004) 296-303.
[5] T. Masuzawa, State of the Art of Micromachining, CIRP Annals - Manufacturing Technology, 49 (2000) 473-488.
[6] L. Romoli, C.A.A. Rashed, G. Lovicu, G. Dini, F. Tantussi, F. Fuso, M. Fiaschi, Ultrashort pulsed laser drilling and surface structuring of microholes in stainless steels, CIRP Annals, 63 (2014) 229-232.
[7] L. Romoli, C.A.A. Rashed, M. Fiaschi, Experimental characterization of the inner surface in micro-drilling of spray holes: A comparison between ultrashort pulsed laser and EDM, Optics & Laser Technology, 56 (2014) 35-42.
[8] B. Adelmann, R. Hellmann, Rapid micro hole laser drilling in ceramic substrates using single mode fiber laser, Journal of Materials Processing Technology, 221 (2015) 80-86.
[9] W.C. Choi, J.Y. Ryu, Fabrication of a guide block for measuring a device with fine pitch area-arrayed solder bumps, Microsyst Technol, 18 (2012) 333-339.
[10] N. Watanabe, M. Suzuki, K. Kawano, M. Eto, M. Aoyagi, Fabrication of a membrane probe card using transparent film for three-dimensional integrated circuit testing, Jpn. J. Appl. Phys., 53 (2014) 06JM06.
[11] W.C. Choi, J.Y. Ryu, A MEMS guide plate for a high temperature testing of a wafer level packaged die wafer, Microsyst Technol, 17 (2011) 143-148.
[12] L. Romoli, R. Vallini, Experimental study on the development of a micro-drilling cycle using ultrashort laser pulses, Optics and Lasers in Engineering, 78 (2016) 121-131.
[13] X.C. Wang, H.Y. Zheng, P.L. Chu, J.L. Tan, K.M. Teh, T. Liu, B.C.Y. Ang, G.H. Tay, Femtosecond laser drilling of alumina ceramic substrates, Applied Physics a-Materials Science & Processing, 101 (2010) 271-278.
[14] A.H. Khan, S. Celotto, L. Tunna, W. O'Neill, C.J. Sutcliffe, Influence of microsupersonic gas jets on nanosecond laser percussion drilling, Optics and Lasers in Engineering, 45 (2007) 709-718.
[15] A.H. Khan, W. O'Neill, L. Tunna, C.J. Sutcliffe, Numerical analysis of gas-dynamic instabilities during the laser drilling process, Optics and Lasers in Engineering, 44 (2006) 826-841.
[16] J.C. Hsu, W.Y. Lin, Y.J. Chang, C.C. Ho, C.L. Kuo, Continuous-wave laser drilling assisted by intermittent gas jets, International Journal of Advanced Manufacturing Technology, 79 (2015) 449-459.
[17] C.C. Ho, Y.M. Chen, J.C. Hsu, Y.J. Chang, C.L. Kuo, Characteristics of the effect of swirling gas jet assisted laser percussion drilling based on machine vision, Journal of Laser Applications, 27 (2015) 042001.
[18] H. Zhang, J. Di, M. Zhou, Y. Yan, R. Wang, An investigation on the hole quality during picosecond laser helical drilling of stainless steel 304, Applied Physics a-Materials Science & Processing, 119 (2015) 745-752.
[19] C. He, F. Zibner, C. Fornaroli, J. Ryll, J. Holtkamp, A. Gillner, High-precision helical cutting using ultra-short laser pulses, Physics Procedia2014, pp. 1066-1072.
[20] N. Iwatani, H.D. Doan, K. Fushinobu, Optimization of near-infrared laser drilling of silicon carbide under water, Int. J. Heat Mass Transf., 71 (2014) 515-520.

[21] V. Nasrollahi, P. Penchev, S. Dimov, L. Korner, R. Leach, K. Kim, Two-Side Laser Processing Method for Producing High Aspect Ratio Microholes, Journal of Micro and Nano-Manufacturing, 5 (2017) 041006-041006-041014.
[22] K. Goya, T. Itoh, A. Seki, K. Watanabe, Efficient deep-hole drilling by a femtosecond, 400 nm second harmonic Ti:Sapphire laser for a fiber optic in-line/pico-liter spectrometer, Sensors and Actuators B-Chemical, 210 (2015) 685-691.
[23] H. Huang, L.-M. Yang, J. Liu, Micro-hole drilling and cutting using femtosecond fiber laser, Optical Engineering, 53 (2014) 051513.
[24] Y. Zhang, Y. Wang, J. Zhang, Y. Liu, X. Yang, W. Li, Effects of Laser Repetition Rate and Fluence on Micromachining of TiC Ceramic, Materials and Manufacturing Processes, (2015).
[25] Y. Zhang, Y. Wang, J. Zhang, Y. Liu, X. Yang, Q. Zhang, Micromachining features of TiC ceramic by femtosecond pulsed laser, Ceram. Int., 41 (2015) 6525-6533.
[26] M. Ghoreishi, O.B. Nakhjavani, Optimisation of effective factors in geometrical specifications of laser percussion drilled holes, Journal of Materials Processing Technology, 196 (2008) 303-310.
[27] M. Ghoreishi, D.K.Y. Low, L. Li, Comparative statistical analysis of hole taper and circularity in laser percussion drilling, International Journal of Machine Tools and Manufacture, 42 (2002) 985-995.
[28] G.K.L. Ng, L. Li, Repeatability characteristics of laser percussion drilling of stainless-steel sheets, Optics and Lasers in Engineering, 39 (2003) 25-33.
[29] S.H. Kim, I.-B. Sohn, S. Jeong, Ablation characteristics of aluminum oxide and nitride ceramics during femtosecond laser micromachining, Applied Surface Science, 255 (2009) 9717-9720.
[30] A. Bharatish, H.N. Narasimha Murthy, B. Anand, C.D. Madhusoodana, G.S. Praveena, M. Krishna, Characterization of hole circularity and heat affected zone in pulsed CO2 laser drilling of alumina ceramics, Optics & Laser Technology, 53 (2013) 22-32.
[31] M.J. Jackson, W. O'Neill, Laser micro-drilling of tool steel using Nd:YAG lasers, Journal of Materials Processing Technology, 142 (2003) 517-525.
[32] A. Schoonderbeek, C.A. Biesheuvel, R.M. Hofstra, K.J. Boller, J. Meijer, The influence of the pulse length on the drilling of metals with an excimer laser, Journal of Laser Applications, 16 (2004) 85-91.
[33] G. Thawari, J.K.S. Sundar, G. Sundararajan, S.V. Joshi, Influence of process parameters during pulsed Nd:YAG laser cutting of nickel-base superalloys, Journal of Materials Processing Technology, 170 (2005) 229-239.
[34] Y. Liu, C. Wang, W. Li, L. Zhang, X. Yang, G. Cheng, Q. Zhang, Effect of energy density and feeding speed on micro-hole drilling in C/SiC composites by picosecond laser, Journal of Materials Processing Technology, 214 (2014) 3131-3140.
[35] D. Dergez, M. Schneider, A. Bittner, U. Schmid, Mechanical and electrical properties of DC magnetron sputter deposited amorphous silicon nitride thin films, Thin Solid Films, 589 (2015) 227-232.
[36] J.M. Liu, Simple technique for measurements of pulsed Gaussian-beam spot sizes, Optics Letters, 7 (1982) 196-198.
[37] V.V. Semak, J.G. Thomas, B.R. Campbell, Drilling of steel and HgCdTe with the femtosecond pulses produced by a commercial laser system, Journal of Physics D: Applied Physics, 37 (2004) 2925-2931.
[38] A. Ruf, P. Berger, F. Dausinger, H. Hügel, Analytical investigations on geometrical influences on laser drilling, Journal of Physics D: Applied Physics, 34 (2001) 2918-2925.

[39] S. Döring, S. Richter, A. Tünnermann, S. Nolte, Evolution of hole depth and shape in ultrashort pulse deep drilling in silicon, Applied Physics A: Materials Science and Processing, 105 (2011) 69-74.
[40] Qioptiq, LINOS F-Theta Ronar fused silica lenses: Custom adaptations to the latest market trends, LASER World of Photonics2013.
[41] B. Xia, L. Jiang, X. Li, X. Yan, Y. Lu, Mechanism and elimination of bending effect in femtosecond laser deep-hole drilling, Optics Express, 23 (2015) 27853-27864.

Figure Captions:

Figure 1. The XCT cross sections of the holes produced with the three lenses by delivering 500, 1000, 5000 and 10000 pulses. Note: all measurements are in microns and were taken employing VG studio 3.0.

Figure 2. Percussion drilling saturation points for the three lenses

Figure 3. The penetration depths achieved with the different fluence levels for the three lenses when 1,000 and 10,000 pulses were used.

Figure 4. The achievable aspect ratios with the different fluence levels for the three lenses when 1,000 and 10,000 pulses were used.

Figure 5. The achieved penetration depth with three lenses when a defocusing is applied, (a) 500 pulses and (b) 5,000 pulses.

Figure 6. Beam spatial profiles of the three lenses at the substrate surface when different levels of defocusing are applied.

Figure 7. The filtered out portions of beam intensity: (a) a focused beam and (b) a negative defocused beam.

Figure 8. Issues with high aspect ratio holes, (a) recasts and (b) bending.

Table Captions

Table 1. Design of experiments for assessing the fluence effects, employing three focusing lenses

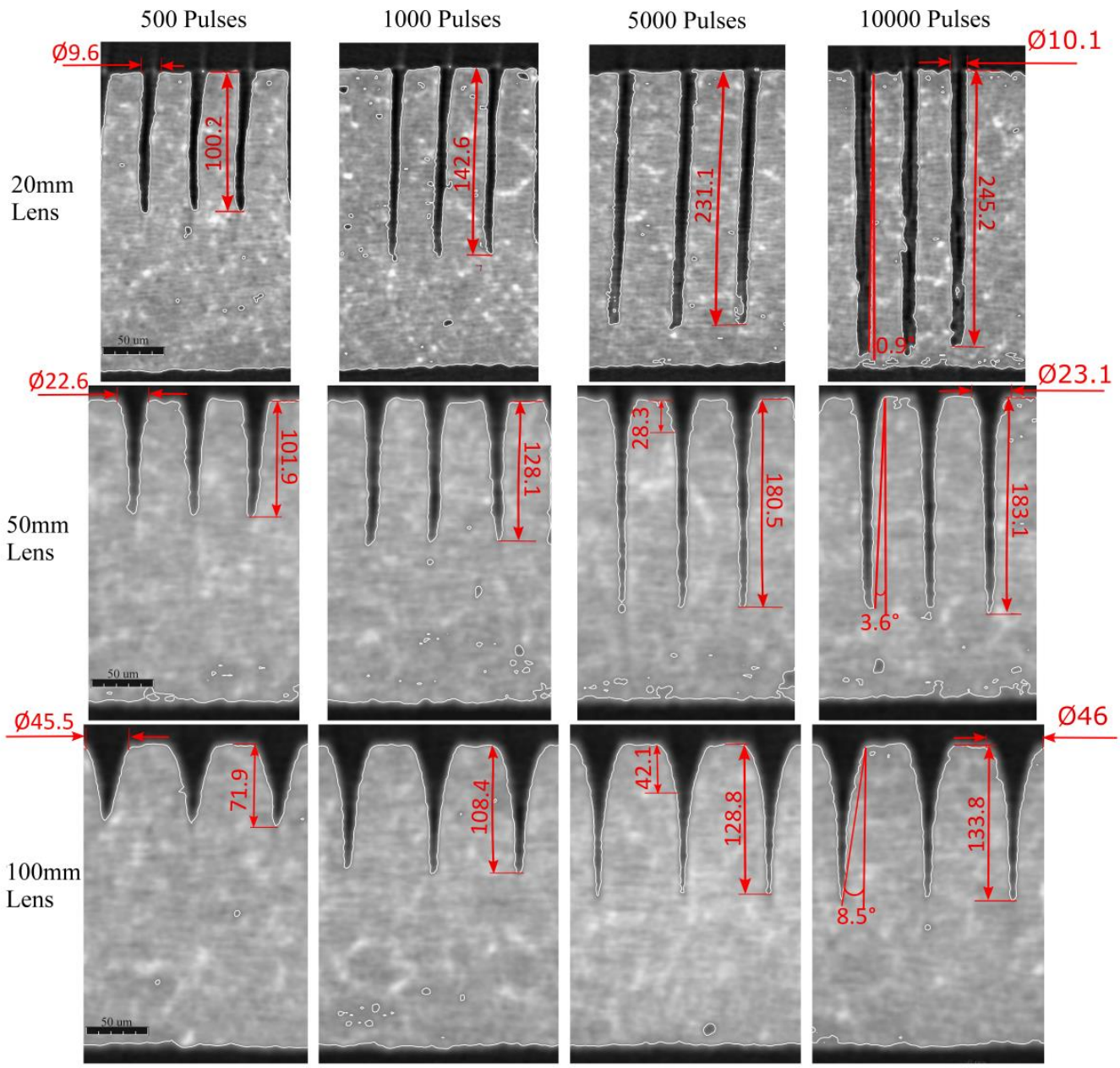

Figure 1. The XCT cross sections of the holes produced with the three lenses by delivering 500, 1000, 5000 and 10000 pulses. Note: all measurements are in microns and were taken employing VG studio 3.0.

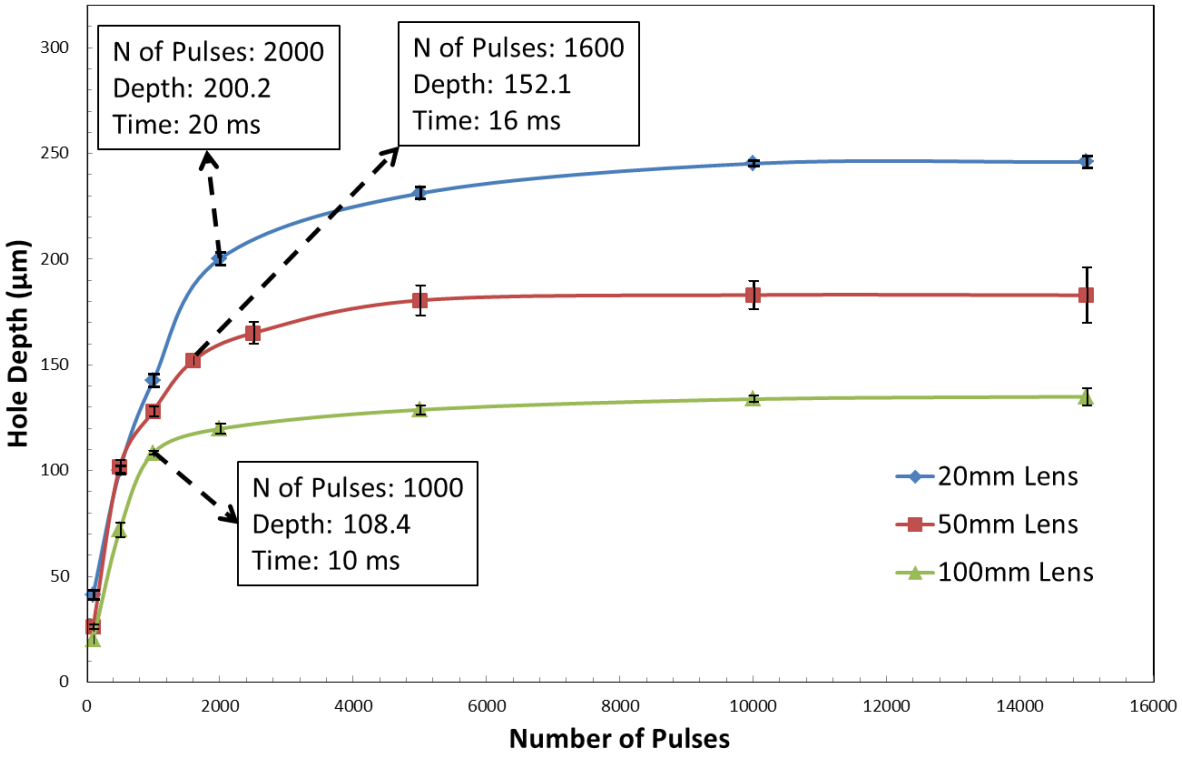

Figure 2. Percussion drilling saturation points for the three lenses

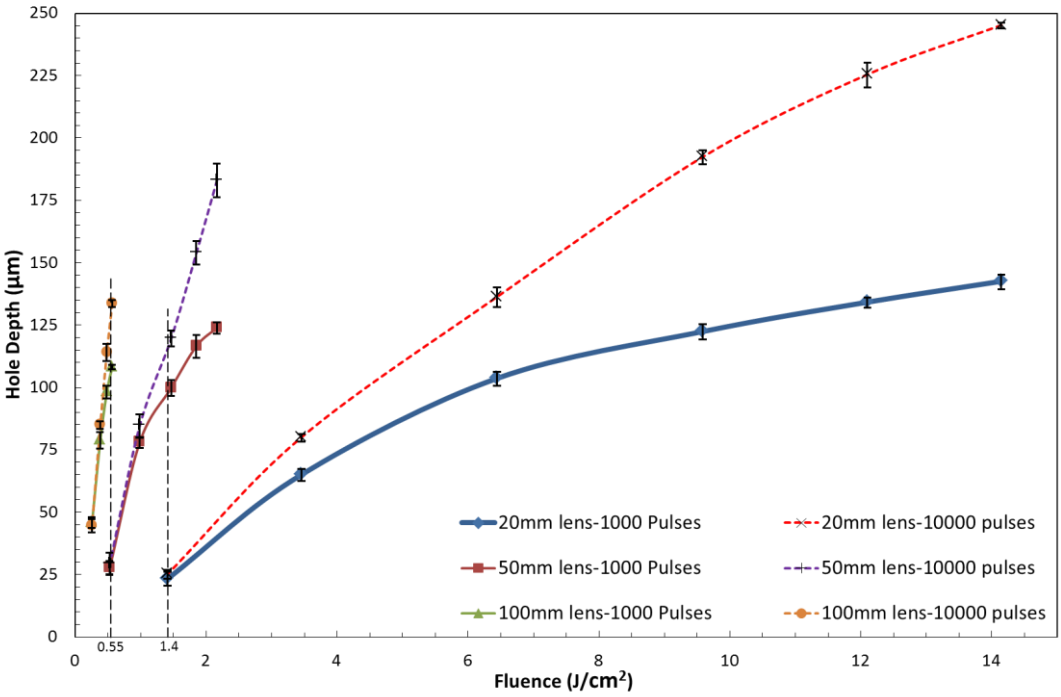

Figure 3. The penetration depths achieved with the different fluence levels for the three lenses when 1,000 and 10,000 pulses were used.

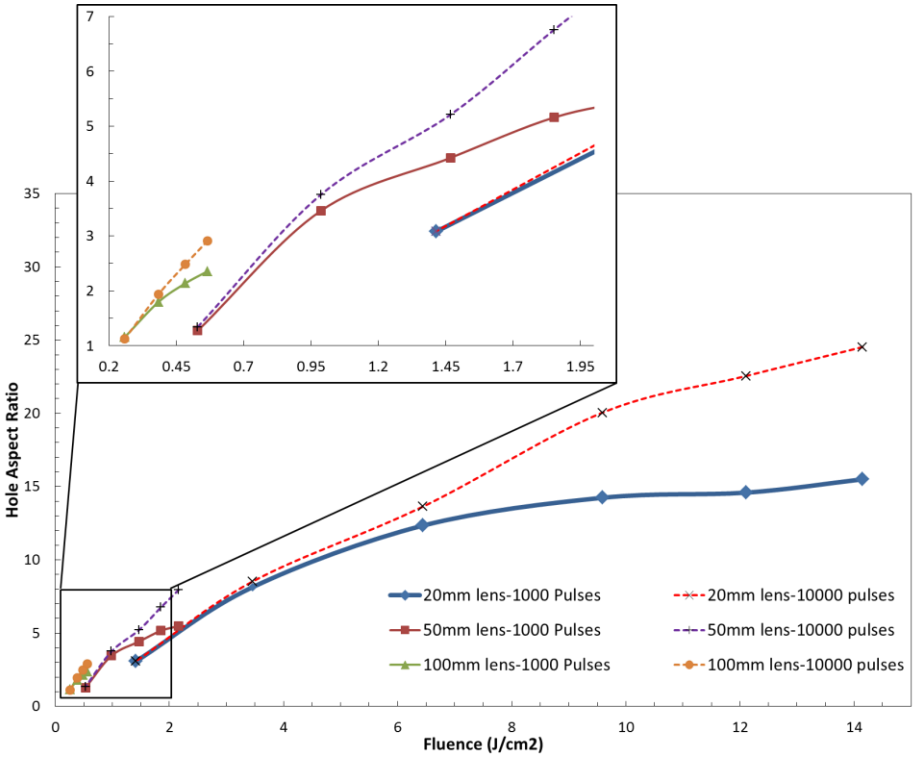

Figure 4. The achievable aspect ratios with the different fluence levels for the three lenses when 1,000 and 10,000 pulses were used.

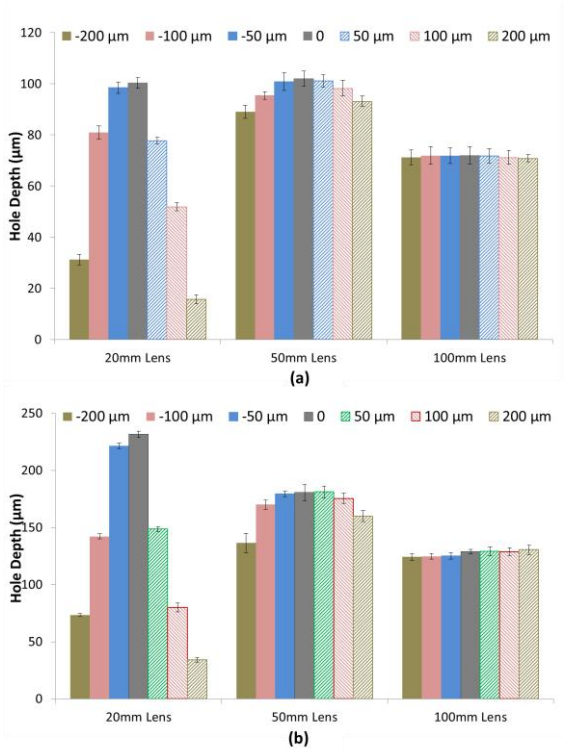

Figure 5. The achieved penetration depth with three lenses when a defocusing is applied, (a) 500 pulses and (b) 5,000 pulses.

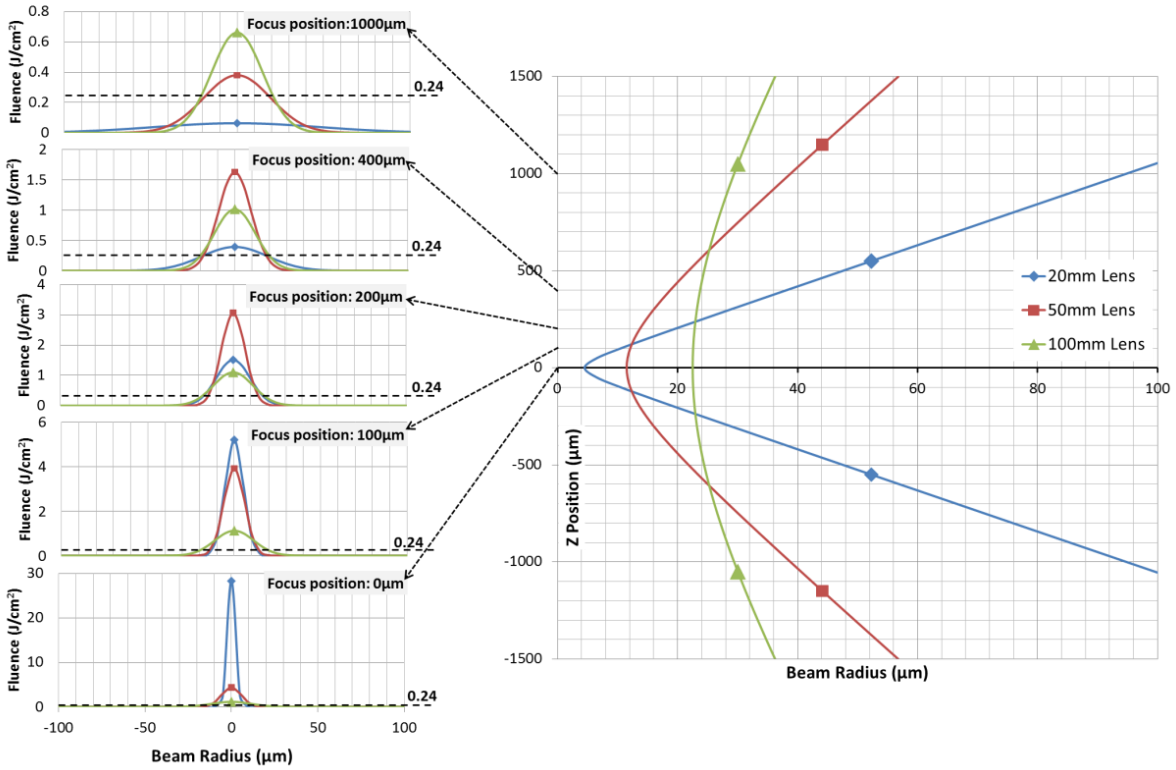

Figure 6. Beam spatial profiles of the three lenses at the substrate surface when different levels of defocusing are applied.

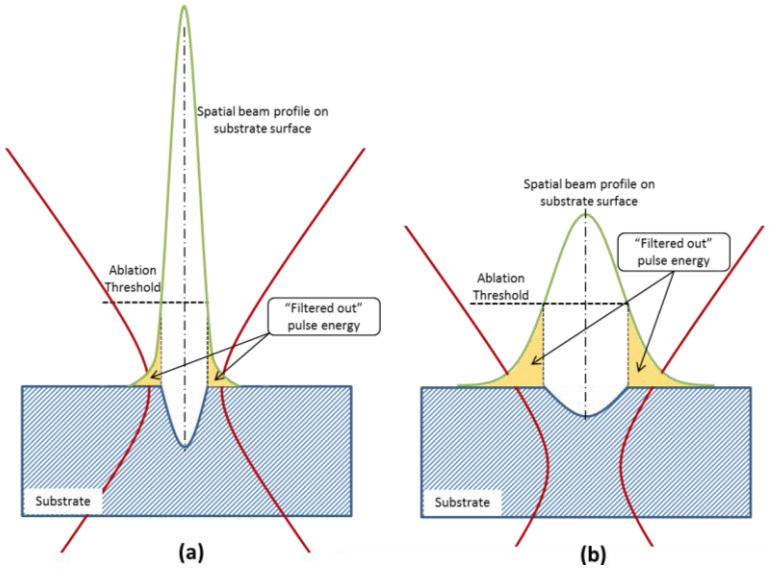

Figure 7. The filtered out portions of beam intensity: (a) a focused beam and (b) a negative defocused beam.

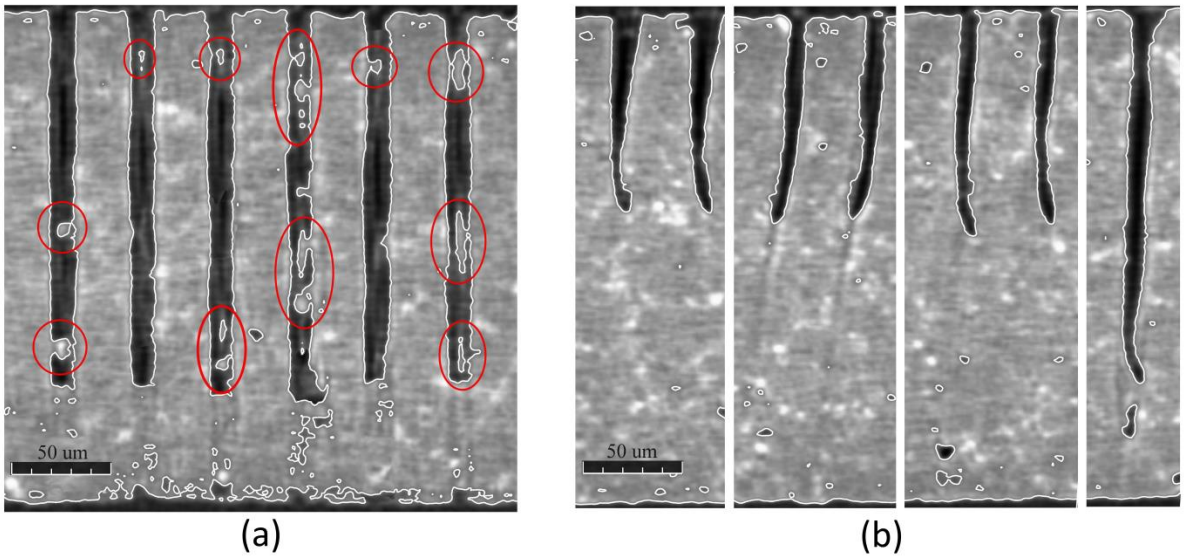

Figure 8. Issues with high aspect ratio holes, (a) recasts and (b) bending.

Table 1. Design of experiments for assessing the fluence effects, employing three focusing lenses

Exp. Trials	Number of Pulses	Pulse Energy	Corresponding Fluence		
			100 mm lens	50 mm lens	20 mm lens
1 to 6	1000, 10000	9 µJ	0.57 J/cm^2	2.17 J/cm^2	14.15 J/cm^2
7 to 12	1000, 10000	7.7 µJ	0.48 J/cm^2	1.85 J/cm^2	12.10 J/cm^2
13 to 18	1000, 10000	6.1 µJ	0.38 J/cm^2	1.47 J/cm^2	9.59 J/cm^2
19 to 24	1000, 10000	4.1 µJ	0.26 J/cm^2	0.99 J/cm^2	6.44 J/cm^2
25 to 28	1000, 10000	2.2 µJ	0.14 J/cm^2	0.53 J/cm^2	3.46 J/cm^2
29 & 30	1000, 10000	0.9 µJ	0.06 J/cm^2	0.22 J/cm^2	1.41 J/cm^2